WILEY-VCH

Edited by
Senentxu Lanceros-Méndez and Pedro Martins

Magnetoelectric Polymer-Based Composites

Fundamentals and Applications

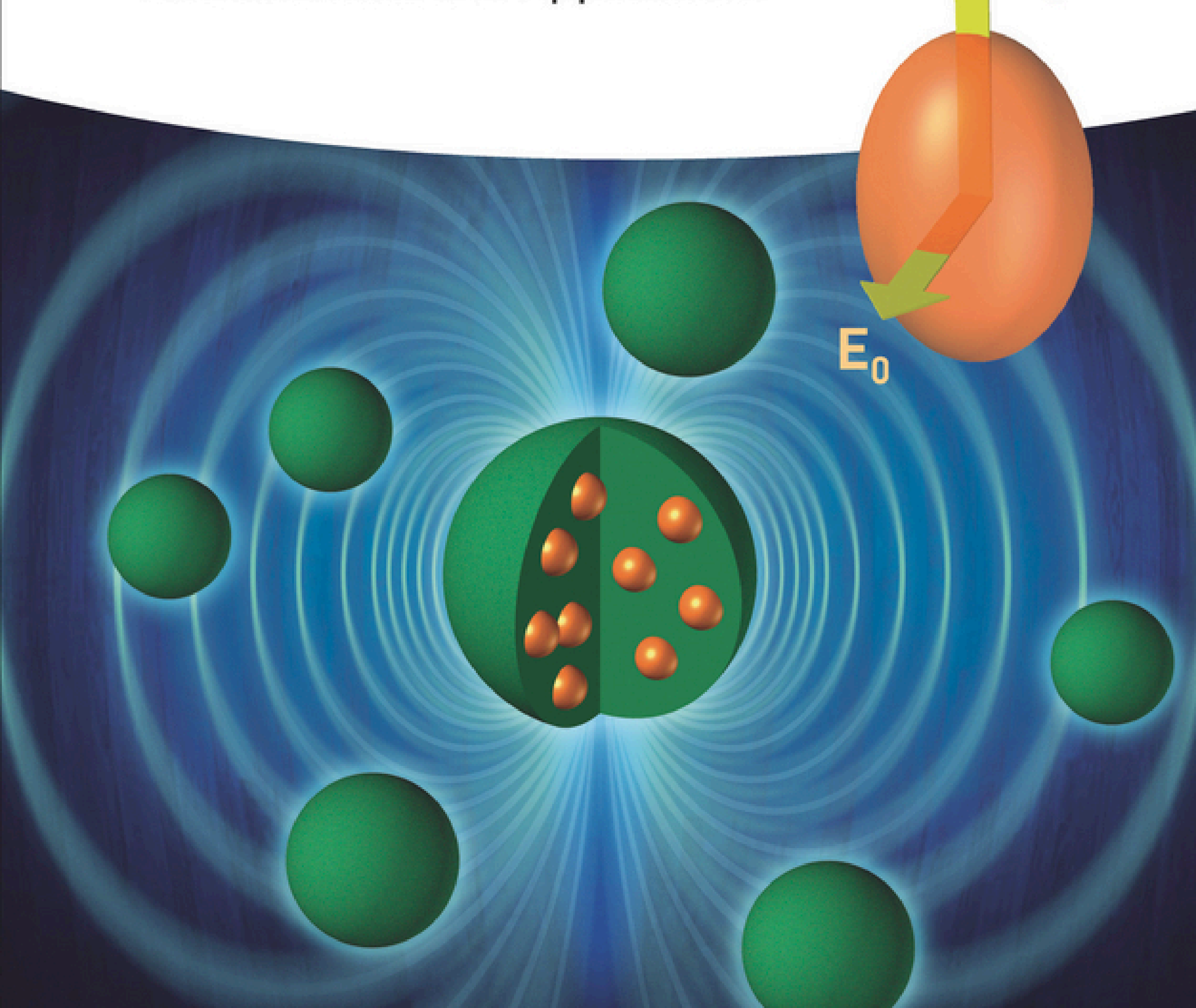

Magnetoelectric Polymer-Based Composites

Magnetoelectric Polymer-Based Composites

Fundamentals and Applications

Edited by Senentxu Lanceros-Méndez and Pedro Martins

WILEY-VCH

Editors

Prof. Senentxu Lanceros-Méndez
Universidade do Minho
Centro de Física
Campus de Gualtar
Braga 4710-057
Portugal

Prof. Pedro Martins
Universidade do Minho
Centro de Física
Campus de Gualtar
Braga 4710-057
Portugal

Library of Congress Card No.: applied for

British Library Cataloguing-in-Publication Data
A catalogue record for this book is available from the British Library.

Bibliographic information published by the Deutsche Nationalbibliothek
The Deutsche Nationalbibliothek lists this publication in the Deutsche Nationalbibliografie; detailed bibliographic data are available on the Internet at <http://dnb.d-nb.de>.

Print ISBN: 978-3-527-34127-6
ePDF ISBN: 978-3-527-80134-3
ePub ISBN: 978-3-527-80135-0
Mobi ISBN: 978-3-527-80136-7
oBook ISBN: 978-3-527-80133-6

Cover Design Schulz Grafik-Design, Fußgönheim, Germany
Typesetting SPi Global, Chennai, India
Printing and Binding

Printed on acid-free paper

Contents

List of Contributors *xi*
Preface and Acknowledgments *xv*

1 Magnetoelectric Effect of Functional Materials: Theoretical Analysis, Modeling, and Experiment *1*
Jia-Wei Zhang, Hong-Yan Guo, Xiao Chen, and Rui-Tong Liu
1.1 Introduction of Magnetoelectric Effect *1*
1.1.1 Single-Phase Magnetoelectric Materials *1*
1.1.2 Multiphase Materials *2*
1.2 Applications of Magnetoelectric Effect *2*
1.2.1 Magnetoelectric Sensors *3*
1.2.2 Magnetoelectric Transducer *3*
1.2.3 Magnetoelectric Microwave Devices *4*
1.3 Magnetoelectric Effect of Piezoelectric Ceramic *4*
1.4 Magnetoelectric Effect in Insulating Polymers *7*
1.5 Conclusion *11*
Acknowledgments *11*
References *11*

2 Materials Selection, Processing, and Characterization Technologies *13*
Jing Ma, Lu Song, Chen Liu, and Chengzhou Xin
2.1 Introduction *13*
2.2 Materials Selection and Processing *14*
2.2.1 Polymer as the Piezoelectric/Ferroelectric Phase *15*
2.2.2 Piezoelectric Polymer as the Matrix *17*
2.2.3 Non-piezoelectric Polymer as the Active Matrix *18*
2.2.4 Polymer as the Binder *18*
2.3 Characterization Technologies *19*
2.3.1 Ferroelectric and Piezoelectric Characterization *19*
2.3.1.1 Piezoelectric Characterization *19*
2.3.1.2 Ferroelectric Characterization *20*
2.3.2 Magnetostrictive and Magnetism Characterization *22*
2.3.2.1 Magnetism Measurement *23*

2.3.2.2 Magnetostriction Measurement *26*
2.3.3 Characterization of Magnetoelectric Coupling *27*
2.3.3.1 Direct Magnetoelectric Coupling *27*
2.3.3.2 Converse Magnetoelectric Coupling *30*
2.4 Concluding Remarks *34*
Acknowledgments *34*
References *34*

3 Types of Polymer-Based Magnetoelectric Materials *45*

3a Laminates *47*
Marco Silva, Pedro Martins, and Senentxu Lanceros-Mendez
3a.1 Introduction *47*
3a.2 Laminated Magnetoelectric Composites *47*
3a.3 Piezoelectric Phase for Magnetoelectric Laminates *53*
3a.3.1 PVDF and Its Copolymers *53*
3a.3.2 Diamines *54*
3.4a Magnetostrictive Phase for Magnetoelectric Laminates *55*
3a.4.1 Metglas *55*
3a.4.2 VITROVAC *57*
3a.4.3 Terfenol-D *57*
3.5a Bonding Agent for Magnetoelectric Laminates *57*
3a.6 Structures for Magnetoelectric Laminates *58*
3a.7 Limitations and Remaining Challenges *59*
Acknowledgments *59*
References *60*

3b Polymer-Based Magnetoelectric Composites: Polymer as a Binder *65*
Yang Song, De'an Pan, Zhijun Zuo, and Alex Alexei Volinsky
3b.1 Introduction *65*
3b.2 Polymer-Based $Tb_{1-x}Dy_xFe_{2-y}$ by Magnetic Warm Compaction *66*
3b.2.1 Experiment for Magnetic Warm Compaction *66*
3b.2.2 Results and Discussion of Magnetic Warm Compaction *67*
3b.2.3 Conclusions for Magnetic Warm Compaction *70*
3b.3 Multifaceted Magnetoelectric Composites *70*
3b.3.1 Experiment for Multifaceted Magnetoelectric Composites *70*
3b.3.2 Results and Discussion for Multifaceted Magnetoelectric Composites *70*
3b.3.3 Conclusions for Multifaceted Magnetoelectric Composites *73*
3b.4 Bonded Cylindrical Composites *73*
3b.4.1 Experiment for Bonded Cylindrical Composites *73*
3b.4.2 Results and Discussion for Bonded Cylindrical Composites *74*
3b.4.3 Conclusions for Bonded Cylindrical Composites *76*
3b.5 Multi-electrode Cylinder Composites *77*
3b.5.1 Experiment for Multi-electrode Cylinder Composites *77*

3b.5.2 Results and Discussion for Multi-electrode Cylinder Composites *78*
3b.5.3 Conclusions for Multi-electrode Cylinder Composites *81*
3b.6 Polymer Content and Particle Size Effects *81*
3b.6.1 Experiment for Polymer Content and Particle Size Effects *81*
3b.6.2 Results and Discussion for Polymer Content and Particle Size Effects *81*
3b.6.3 Conclusions for Polymer Content and Particle Size Effects *83*
Acknowledgments *84*
References *84*

3c Poly(vinylidene fluoride)-Based Magnetoelectric Polymer Nanocomposite Films *87*
Thandapani Prabhakaran and Jawaharlal Hemalatha
3c.1 Introduction *87*
3c.2 Ferroelectric Polymers *89*
3c.2.1 Poly(Vinylidene Fluoride) *90*
3c.2.2 Crystallization of β-Phase PVDF *91*
3c.2.2.1 By Solvent *91*
3c.2.2.2 By the Temperature *91*
3c.2.2.3 Electric Poling on PVDF *92*
3c.3 The Selection of Magnetic Nanofillers *93*
3c.4 Experimental Methods *94*
3c.4.1 Materials *94*
3c.4.2 Synthesis of Magnetic Nanoparticles *95*
3c.4.3 Fabrication of ME Polymer Nanocomposites *95*
3c.5 Characterization *96*
3c.5.1 IR Vibrational Studies *96*
3c.5.2 Surface Analysis on the Composites *98*
3c.5.3 Magnetic Studies on MPNCs *100*
3c.5.4 Correlation of $F(\beta)$ with Ferroelectric Parameters *102*
3c.5.5 Magnetoelectric Effect in MPNCs *102*
3c.6 Summary *107*
3c.7 Future Directions *108*
Acknowledgments *109*
References *109*

4 Low-Dimensional Polymer-Based Magnetoelectric Structures *115*
Renato Gonçalves, Senentxu Lanceros-Mendez, and Pedro Martins
4.1 Introduction *115*
4.2 Magnetoelectric Spheres *117*
4.3 Magnetoelectric Fibers *118*
4.4 Magnetoelectric Membranes *119*
4.5 Conclusions and Future Perspectives *120*
Acknowledgments *121*
References *122*

5 Design of Magnetostrictive Nanoparticles for Magnetoelectric Composites *125*
Victor Sebastian
5.1 Introduction *125*
5.1.1 Magnetoelectric Composites *125*
5.1.2 Magnetostriction and Magnetostrictive Materials *126*
5.1.3 Ferromagnetic Ferrites *129*
5.1.4 Ferroelectric Perovskites *131*
5.2 Synthesis Approaches to Produce Magnetostrictive Nanoparticles for Magnetoelectric Composites *132*
5.2.1 Top-Down Production Approaches *133*
5.2.1.1 Mechanosynthesis or Mechanical Attrition *133*
5.2.1.2 Mechanical Alloying *134*
5.2.1.3 Inert-Gas Condensation Approach *134*
5.2.2 Bottom-Up Production Approaches *135*
5.2.2.1 Solid-State Reaction *135*
5.2.2.2 Pyrolysis *136*
5.2.2.3 Wet-Chemical Approaches *137*
5.3 Summary and Future Perspectives *145*
Acknowledgments *146*
References *146*

6 Applications of Polymer-Based Magnetoelectric Materials *153*

6a Sensors, Actuators, Antennas, and Memories *155*
Sílvia Reis, Marco Silva, Pedro Martins, and Senentxu Lanceros-Mendez
6a.1 Introduction *155*
6a.2 Polymer-Based Magnetoelectric Sensors *156*
6a.3 Polymer-Based Magnetoelectric Actuators *159*
6a.4 Polymer-Based Magnetoelectric Antennas *161*
6a.5 Polymer-Based Magnetoelectric Memories *164*
6a.6 Opportunities, Limitations, and Remaining Challenges *165*
Acknowledgments *166*
References *166*

6b Magnetoelectric Composites for Bionics Applications *171*
Tian Zheng, Yan Zong, Zhilian Yue, Gordon G. Wallace, and Michael J. Higgins
6b.1 Introduction *171*
6b.2 Bionics *171*
6b.2.1 Implantable Electrode Devices *171*
6b.2.2 Organic Electrode Materials *172*
6b.2.3 New Opportunities for Advanced Electrical Stimulation *173*
6b.3 Cell Interactions and Electrical Stimulation *175*
6b.3.1 Synthetic Polymer-Based ME *175*
6b.3.2 Nanostructured and Nanoscale ME Materials *177*

6b.3.3 ME Concept for Electrical Stimulation of Cells *179*
6b.4 Future Biomaterials for ME Composites *180*
6b.4.1 Piezoelectric DNA, Proteins, and Microorganisms *180*
6b.4.2 ME Biopolymers: Cellulose *182*
6b.5 Characterization Tools for Nanoscale ME *184*
6b.5.1 Piezoresponse Force Microscopy (PFM) *184*
6b.5.2 Bio-Atomic Force Microscopy (Bio-AFM) *187*
Acknowledgments *188*
References *189*

6c Energy Harvesting *197*
Chess Boughey and Sohini Kar-Narayan
6c.1 Introduction *197*
6c.2 Magnetoelectric Composites for Energy Harvesting *198*
6c.2.1 Magnetostrictive Effect in Ferromagnetic Materials *200*
6c.2.2 Piezoelectricity in Polymers *201*
6c.2.3 Key Parameters, Equations, and Figures of Merit *205*
6c.2.4 Magnetoelectric Effect in Piezoelectric–Ferromagnetic Composites *208*
6c.3 Energy-Harvesting Devices Based on Magnetoelectric Composites *211*
6c.4 Conclusion *212*
References *215*

6d High-Temperature Polymers for Magnetoelectric Applications *225*
Alberto Maceiras, José Luis Vilas, and Luis Manuel León
6d.1 Introduction *225*
6d.2 Types of Piezoelectric Polymers *226*
6d.2.1 Piezocomposites *226*
6d.2.2 Ferroelectrets *226*
6d.2.3 Bulk Piezoelectric Polymers *229*
6d.2.3.1 Semicrystalline Piezoelectric Polymers *229*
6d.2.3.2 Amorphous Piezoelectric Polymers *235*
6d.3 ME Effect Using Piezoelectric Polyimides *240*
6d.4 Summary and Conclusions *241*
References *242*

7 Open Questions, Challenges, and Perspectives *255*
Pedro Martins and Senentxu Lanceros-Mendez
References *258*

Index *259*

List of Contributors

Chess Boughey
University of Cambridge
Department of Materials Science & Metallurgy
27 Charles Babbage Road
Cambridge CB3 0FS
UK

Xiao Chen
Northeast Electric Power University
School of Electrical Engineering
169 Changchun Road
Jilin 132013
China

Renato Gonçalves
Universidade do Minho
Departamento de Física
4710-057 Braga
Portugal

Hong-Yan Guo
Northeast Electric Power University
School of Electrical Engineering
169 Changchun Road
Jilin 132013
China

Jawaharlal Hemalatha
National Institute of Technology
Advanced Materials Lab
Department of Physics
Tiruchirappalli
Tamilnadu 620015
India

Michael J. Higgins
University of Wollongong
ARC Centre of Excellence for Electromaterials Science
Intelligent Polymer Research Institute/AIIM Faculty
Innovation Campus
Squires Way
NSW 2522
Australia

Sohini Kar-Narayan
University of Cambridge
Department of Materials Science & Metallurgy
27 Charles Babbage Road
Cambridge CB3 0FS
UK

Senentxu Lanceros-Mendez
Universidade do Minho
Centro de Física
Campus de Gualtar
Braga 4710-057
Portugal

and

BCMaterials, Basque Center for Materials
Applications and Nanostructures
Parque Científico y Tecnológico de Bizkaia
Bld 500, 48160 Derio
Spain

and

IKERBASQUE
Basque Foundation for Science
Maria Diaz de Haro 3
48013 Bilbao
Spain

Luis Manuel León
University of the Basque Country (UPV/EHU)
Macromolecular Chemistry Research Group (LABQUIMAC)
Department of Physical Chemistry
Faculty of Science and Technology
Spain

and

BCMaterials, Basque Center for Materials, Applications and Nanostructures
Parque Científico y Tecnológico de Bizkaia
Bld 500, 48160 Derio
Spain

Chen Liu
Tsinghua University
School of Materials Science and Engineering, and State Key Lab of New Ceramics and Fine Processing
Beijing 100084
China

Jing Ma
Tsinghua University
School of Materials Science and Engineering, and State Key Lab of New Ceramics and Fine Processing
Beijing 100084
China

Alberto Maceiras
University of the Basque Country (UPV/EHU)
Macromolecular Chemistry Research Group (LABQUIMAC)
Department of Physical Chemistry
Faculty of Science and Technology
Spain

Pedro Martins
Universidade do Minho
Centro de Física
Campus de Gualtar
Braga 4710-057
Portugal

De'an Pan
Beijing University of Technology
Institute of Circular Economy
100 Ping Le Yuan
Beijing 100124
China

Thandapani Prabhakaran
National Institute of Technology
Advanced Materials Lab
Department of Physics
Tiruchirappalli
Tamilnadu 620015
India

Sílvia Reis
Universidade do Minho
Departamento de Física
Braga 4710-057
Portugal

Victor Sebastian
University of Zaragoza
Institute of Nanoscience of Aragon
R+D Building
C/Mariano Esquillor, s/n
Zaragoza 50018
Spain

and

Networking Research Center on
Bioengineering, Biomaterials and
Nanomedicine
CIBER-BBN
Madrid 28029
Spain

and

University of Zaragoza
Department of Chemical Engineering
and Environmental Technology
Zaragoza
Spain

Marco Silva
Universidade do Minho
Centro de Física
Campus de Gualtar
Braga 4710-057
Portugal

Lu Song
Tsinghua University
School of Materials Science and
Engineering, and State Key Lab of
New Ceramics and Fine Processing
Beijing 100084
China

Yang Song
University of Science and Technology
Beijing
Department of Mechanical
Engineering
Institute for Advanced Materials and
Technology
30 Xueyuan Road
Beijing 100083
China

and

University of South Florida
College of Engineering
Department of Mechanical
Engineering
4202 E Fowler Ave
Tampa, FL 33620
USA

José Luis Vilas
University of the Basque Country
(UPV/EHU)
Macromolecular Chemistry Research
Group (LABQUIMAC)
Department of Physical Chemistry
Faculty of Science and Technology
Spain

and

BCMaterials, Basque Center for
Materials, Applications and
Nanostructures
Parque Científico y Tecnológico de
Bizkaia
Bld 500, 48160 Derio
Spain

Alex Alexei Volinsky
University of South Florid
College of Engineering
Department of Mechanical Engineering
Tampa, FL 33620
USA

Gordon G. Wallace
University of Wollongong
ARC Centre of Excellence for Electromaterials Science
Intelligent Polymer Research Institute/AIIM Faculty
Innovation Campus, Squires Way
NSW 2522
Australia

Chengzhou Xin
Tsinghua University
School of Materials Science and Engineering, and State Key Lab of New Ceramics and Fine Processing
Beijing 100084
China

Zhilian Yue
University of Wollongong
ARC Centre of Excellence for Electromaterials Science
Intelligent Polymer Research Institute/AIIM Faculty
Innovation Campus, Squires Way
NSW 2522
Australia

Jia-Wei Zhang
Northeast Electric Power University
School of Electrical Engineering
169 Changchun Road
Jilin 132013
China

and

Harbin University of Science and Technology Key Laboratory of Engineering Dielectric and its Application of Ministry of Education
Harbin
China

Tian Zheng
University of Wollongong
ARC Centre of Excellence for Electromaterials Science
Intelligent Polymer Research Institute/AIIM Faculty
Innovation Campus, Squires Way
NSW 2522
Australia

Yan Zong
University of Wollongong
ARC Centre of Excellence for Electromaterials Science
Intelligent Polymer Research Institute/AIIM Faculty
Innovation Campus, Squires Way
NSW 2522
Australia

Zhijun Zuo
Functional Materials Research Institute
Central Iron and Steel Research Institute
No. 76 Xueyuan South Road
Beijing 100081
China

Preface and Acknowledgments

> In every branch of knowledge the progress is proportional to the amount of facts on which to build, and therefore to the facility of obtaining data.
> James Clerk Maxwell (1831–1879)

This book was motivated by the desire for providing a suitable and complete account of the evolution, state of the art, and main challenges of the interesting and growing field of polymer-based magnetoelectric (ME) materials. In this scope, an overview of the frontline research of this fascinating research field has been presented by selected authors with innovative and preponderant work.

The book provides an introduction to polymer-based ME materials and their physicochemical insights, design for technological applications, and implementation into devices.

Chapter 1 deals with the theoretical analysis and modeling of the ME effect of functional materials. The ME effect and its application in single crystal, multilayered composites, and piezoelectrics under the Lorentz force induced by eddy currents have been discussed.

Chapter 2 deals with materials selection, processing, and characterization technologies. Almost two decades of research, innovation, and development on different systems with various compositions and structures are summarized.

Chapter 3 comprises three contributions toward the different types of polymer-based ME materials that we can find in the literature: laminates, *polymer "as a binder*," and nanocomposites. Many exciting results are presented, new concepts are addressed, and future studies are suggested to be carried out for further research on these scientifically interesting and industrially relevant materials.

In the same line, Chapter 4 focuses on the new opportunities and challenges that low dimensionality offers to the nanocomposite structure.

The subject of Chapter 5 is the design of magnetostrictive nanoparticles for ME composites. This chapter focuses on those nanomaterials that, after being coupled to a piezoelectric polymer matrix, can provide unique ME responses.

Chapter 6 presents three contributions concerning the applications of polymer-based ME materials: sensors and actuators, biomedical materials, energy harvesters, and high-temperature devices are presented and discussed. With this application-oriented chapter, it is intended to provide an overview of the ME effect-based devices, the figures of merit, and the problems concerning materials selection, applicability, and design considerations.

Finally, Chapter 7 indicates some of the open questions, challenges, and perspectives of this research field.

This book would have not been possible without the dedicated and insightful work of the authors of the different chapters. The editors truly thank the kindness, dedication, and excellence in providing the different high-quality chapters that show the strength, direction, dimension, and potential of the world of ME polymer-based materials. Truly thanks for sharing with us this important landmark in the area!

This book could have not also been possible without the continuous support, dedication, and understanding from our colleagues from the Electroactive Smart Materials Group of the Center of Physics, University of Minho, Portugal, and from the research group at the BCMaterials, Basque Center for Materials, Applications, and Nanostructures, Leioa, Spain. Thank you all for working together, sharing knowledge together, growing together, and living together as a Group!

Last but not least, we truly thank the team from Wiley for their excellent support: from the first contacts with Jolke Perelaer to the last with Samanaa Srinivas and Sujisha Kunchi Parambathu, passing through the different colleagues who supported this work; their kindness, patience, technical expertise, ideas, perspectives, and insights were essential to make this book come true. We are deeply grateful to them for their generous assistance.

Let us hope this book fulfills its purpose of bringing together the best and most relevant issues on polymer-based ME materials, allowing for a deeper understanding, and pointing out the main challenges and directions for the near future so that we together contribute to a bright future of innovation and implementation in this relevant field!

Braga, Portugal *Pedro Martins and Senentxu Lanceros-Mendez*

1

Magnetoelectric Effect of Functional Materials: Theoretical Analysis, Modeling, and Experiment

Jia-Wei Zhang[1,2], Hong-Yan Guo[1], Xiao Chen[1], and Rui-Tong Liu[3]

[1] Northeast Electric Power University, School of Electrical Engineering,169 Changchun Road, Jilin 132013, China
[2] Harbin University of Science and Technology, Key Laboratory of Engineering Dielectric and its Application of Ministry of Education, Harbin, China
[3] State Grid Liaoning Province Power Company Limited Power Research Institute, Shenyang 110181, China

1.1 Introduction of Magnetoelectric Effect

Magnetoelectric (ME) effect is defined as an induced dielectric polarization under an applied magnetic field and/or an induced magnetization under an external electric field [1]. Materials with ME properties are called magnetoelectric materials (MMs). There are single- and multiphase MMs. Single-phase MMs contain only one type of structure. Little research has been done on single-phase MMs because the intrinsic ME coupling in single-phase compounds is generally quite weak, especially at room temperature. The ME effect in multiphase composite materials is the product of ferromagnetic magnetostriction and ferroelectric piezoelectricity [2].

1.1.1 Single-Phase Magnetoelectric Materials

Single-phase materials possessing both antiferromagnetic and ferroelectric constituents in the same phase are the first discovered ME materials. In 1894, Pierre Curie predicted the possibility of an intrinsic ME effect in some single-phase materials. Although the terminology "magnetoelectric effect" was defined by Debye in 1926, it remained a speculation until 1960 when the first real MM Cr_2O_3 was discovered [3]. In 1969, Homreich discovered some candidates of MMs based on the magnetic point group, including Fe_2TeO_6, Cr_2TeO_6, $FeCrWO_6$, Cr_2WO_6, Ca_2FeAlO_5, and $FeNaO_2$. In 1970, $BiFeO_3$ was found to be unique among various ME multiferroics because of its exceptionally high antiferromagnetic and ferroelectric transition temperatures well above room temperature [4]. An important breakthrough in 2003 was the discovery of large room-temperature ferroelectric polarization in coexistence with magnetization in $BiFeO_3$ thin films, which presents a theoretical investigation on $BiFeO_3$ bulks, films, and heterostructures.

Magnetoelectric Polymer-Based Composites: Fundamentals and Applications, First Edition.
Edited by Senentxu Lanceros-Méndez and Pedro Martins.

1.1.2 Multiphase Materials

In the past century, to overcome the drawbacks of weak ME effect in single-phase materials, ME materials have evolved from single-phase compounds to multiphase materials. Multiphase materials are usually prepared by combining ferromagnetic and ferroelectric phases in the bulk and laminated forms.

In 1948, Tellegen failed to synthesize bulk composites with extrinsic ME effect by combining two different types of macroscopic particle composites with magnetic and electric dipole moments as the beginning of the investigation. In the early 1990s, bulk composites of ferrites and $BaTiO_3$ or Pb(Zr, Ti)O_3 (PZT) had been prepared by Newnham's group and Russian scientists through a conventional sintering process. In 2001, Patankar *et al.* performed extended experiments on several doped ferrite/titanate bulk composites such as $CuFe_{1.8}Cr_{0.2}O_4/Ba_{0.8}Pb_{0.2}TiO_3$. Recently, experiments on many doped titanate/ferrite composites were reported. The piezoelectric constituents include $Bi_4Ti_3O_{12}$, polyvinylidene fluoride (PVDF), $PbMg_{1/3}V_{2/3}O_3$, and $PbX_{1/3}Nb_{2/3}O_3$-$PbTiO_3$ (X = Mg, Zn), and the alternative magnetostrictive constituents include $LiFe_5O_8$, yttrium iron garnet (YIG), and Permendur [5].

Laminated composites are typically made of magnetostrictive material layers bonded with piezoelectric material layers with different arrangements of the magnetization and polarization directions. Figure 1.1 shows an example of the epoxy-bonded-type three-phase laminated composites constructed by sandwiching a thickness-polarized PZT plate between two length-magnetized epoxy-bonded Terfenol-D particulate composite plates [7].

Recently, the direct-coupling Lorentz force effect in the metallic phase with the piezoelectric effect in the piezoelectric phase induced by an extrinsic "dc" ME effect was observed in metallic/piezoelectric heterostructures. Guiffard *et al.* developed an ME current sensor with ME coupling in a simple piezoelectric unimorph bender induced by the eddy currents within the silver electrodes of the piezoelectric ceramic PZT subjected to ac magnetic flux [8]. Therefore, the MMs without the magnetic phase can be used in ME current sensors.

1.2 Applications of Magnetoelectric Effect

So far bulk composites, laminated composites, and metallic/piezoelectric heterostructures exhibit practically useful ME effect above room temperature.

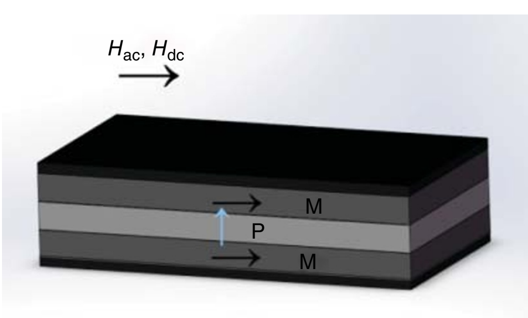

Figure 1.1 Schematic of proposed laminated composites configuration of magnetostrictive and piezoelectric materials [6].

Nowadays, there are some main promising device applications, including ME sensors, ME transducers, ME microwave devices, and so on.

1.2.1 Magnetoelectric Sensors

In the work of Leung *et al.*, a high-sensitive magnetoelectric sensor was obtained using ME composites by increasing the corresponding ME voltage coefficient of 27 mV Oe^{-1} during measurement [9].

The working principle of the sensor was as follows: when an ac vortex magnetic field was induced along the length of the electric cable by an ac electric current in the cable in accordance with Ampère's law, the sensor transduced the ac vortex magnetic field to an ac electric voltage based on the giant ME effect.

1.2.2 Magnetoelectric Transducer

Today, the magnetoelectric transducer has become a hot research topic, partly because the energy harvest from the environment has been considered to be a significant investigation by researchers. There are four main types of vibration energy harvesters (VEHs), namely electrostatic, piezoelectric, ME, and electromagnetic (EM) [10].

The VEH that consisted of a ME/EM composite transducer, a cantilever beam, and magnetic circuits was reported by Qiu and coworkers. The schematic diagram of the proposed ME/EM composite VEH is shown in Figure 1.2a. The ME/EM composite transducer was placed at the tip of the cantilever beam and could act as masses, which lowered the natural frequency of the cantilever beam and scavenged lower frequency vibration energy from environments more effectively. The schematic diagram of the ME/EM composite transducer is shown in Figure 1.2b. The transducer was made up of a coil and a three-phase laminate, which is composed of two Terfenol-D layers and a piezoelectric layer.

The working principle of the ME/EM composite transducer is as follows: based on Faraday's law of electromagnet induction, when the composite transducers undergo alterations of magnetic flux gradient generated by a vibration source,

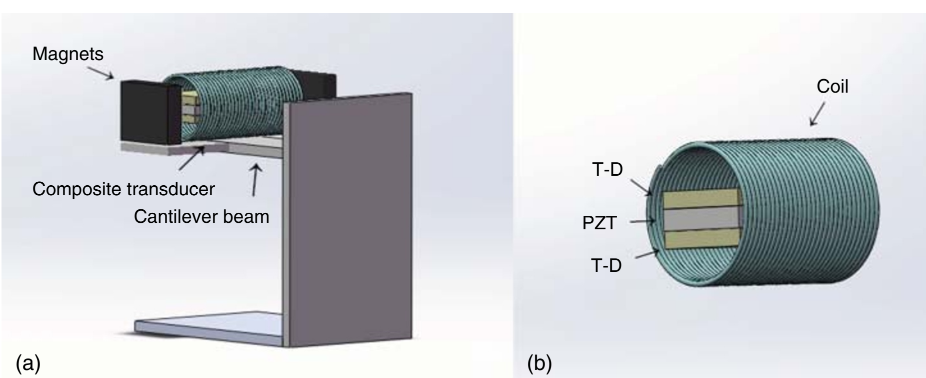

Figure 1.2 Schematic diagrams of (a) the proposed ME/EM composite VEH and (b) the ME/EM composite transducer [10].

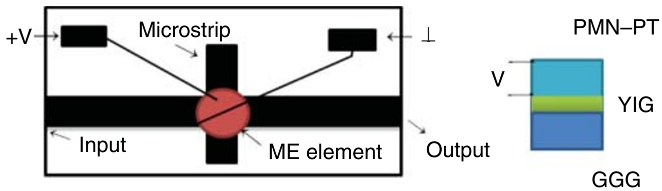

Figure 1.3 Design of microstrip ME attenuator and ME resonator [13]. Tatarenko and Bichurin 2012 https://www.hindawi.com/journals/acmp/2012/286562/abs/. Used under CC BY 3.0 license.

the coil would induce an electromotive force due to the relative motion between the coil and the magnetic circuit. Meanwhile, based on the ME effect, the stresses induced by Terfenol-D layers would transmit to the piezoelectric layer, and finally the electrical power is generated.

1.2.3 Magnetoelectric Microwave Devices

Magnetoelectric microwave devices are the devices that can be tuned by magnetostatic field and electrostatic field when the devices are applied with composited MMs. Because of the advantages of low power consumption, low noise, and high-quality factor, the ME microwave devices have great potential in mobile communication system, electronic warfare systems, active phased-array radar under the national defense platform, and so on [11].

The attenuator with a microstrip transmission line on dielectric substrate and ME resonator was reported by Tatarenko *et al.* With the influence of an external electrical field, the ME effect shifted the line of FMR (ferromagnetic resonance), which is a powerful tool for the studies of microwave ME interaction in ferrite-piezoelectric structures [12].

As shown in Figure 1.3, the sample of layered structure consisted of the magnetic part with the YIG thin film placed on the GGG film and the piezoelectric part with the thin PMN–PT plate. Based on resonance ME effect phenomena, when applying the control voltage to electrodes of the ME resonator, a shift of FMR line would occur due to the resonance ME effect, and hence electrical tuning is realized.

1.3 Magnetoelectric Effect of Piezoelectric Ceramic

Previous reports of magnetoelectric materials with magnetostrictive/piezoelectric magnetoelectric laminates have been discussed by many researchers. However, it requires ac current supply on the electrically conductive Terfenol-D strips. Recently, the ME effect in the piezoelectric beam based on torque moment, which is generated from Lorentz force on the electrodes without magnetic phase in the sample and also without applying power source on the piezoelectric beam, has been reported by Zhang *et al.*

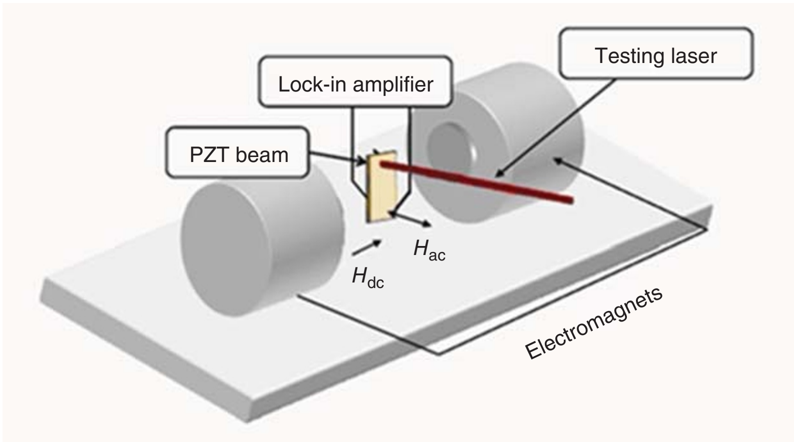

Figure 1.4 Schematic drawing of the experimental system of ME actuator and its torsion velocity measurement [14].

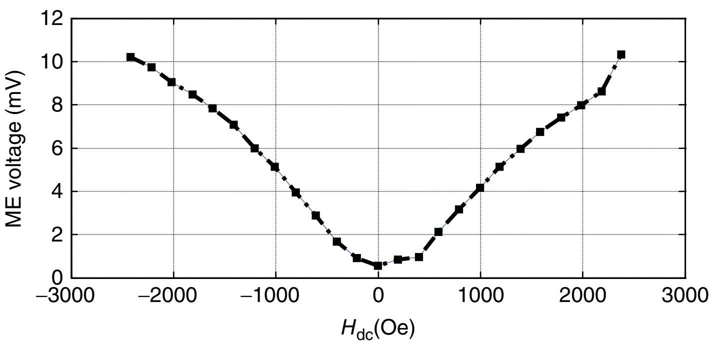

Figure 1.5 Torsion velocity of PZT beam versus the same dc magnetic field.

As shown in Figure 1.4, the measuring system was composed of a PZT beam and an electric wire, which induced the ac magnetic field that penetrated into the surface of the PZT beam. When the metal electrodes of the PZT beam were subjected to ac magnetic fields with suitable directions, frequency, and amplitude, the moment appearing in the sample surface would apply the Lorentz torque force, and thus the mangetoelectric voltage was generated. The lock-in amplifier was used for measuring the induced ME voltage at room temperature. The torsion velocity measurement was performed on the sample by using a laser vibrometer system composed of laser controller and a laser sensor head to prove that the apparent ME effect was a coupled magnetic and electrical phase through mechanical interaction. Figures 1.5 and 1.6 show a linear ME response that the voltage and torsion velocity of PZT beam are proportional to H_{dc} when 1 Oe ac magnetic field is applied with a constant frequency of 480 Hz (resonance frequency of piezoelectric beam).

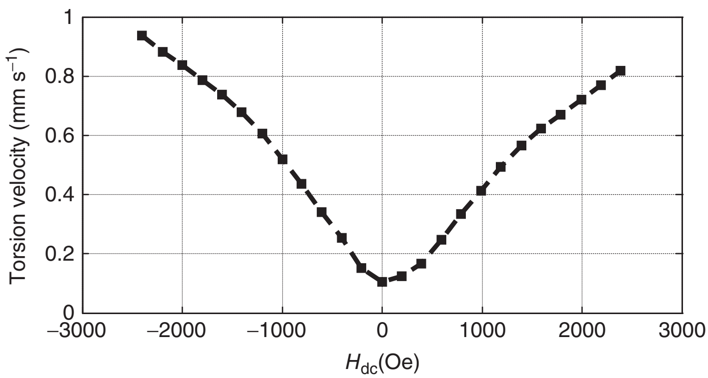

Figure 1.6 Torsion velocity of PZT beam versus the same dc magnetic field.

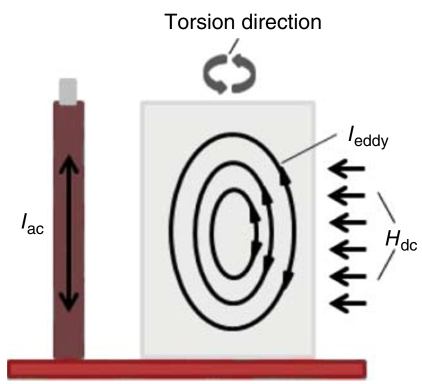

Figure 1.7 Schematic diagram of the rectangular shape piezoelectric beam subjected to ac and dc magnetic fields.

In this experiment, the result of the linear ME response can be explained as that the magnitude of dc magnetic field from 0 to ±2400 Oe was proportional to the magnitude of the moment on the metal layer due to enhanced eddy current. From the aforementioned phenomenon, the ME response would be enhanced by increasing the torsion deformation, which is induced by the moment. Therefore, the generalized ME response without magnetic phase and also without applying power source in the measuring system was observed.

In addition, in order to explore the ME effect in piezoelectric ceramic and the application of ME sensor, the investigation with magnetic actuator has also been developed by Zhang *et al.*

As shown in Figure 1.7, the measuring system for investigating the ME response and torsion deformation of the beam was composed of a piezoelectric beam, an electromagnet, and an ac conducting wire, which induced the ac magnetic flux that penetrated into the metal part of the sample to generate eddy current. Due to the coupling of the piezoelectric layer and Lorentz force from the eddy current, piezoelectric bender's torsion deformation could be induced by Lorentz force, and thus piezoelectric voltage appeared on the sample [15].

As shown in Figures 1.8 and 1.9, the experimental results of PZT bender's voltage and the velocity and an approximate linear relation of ME voltage and torsion

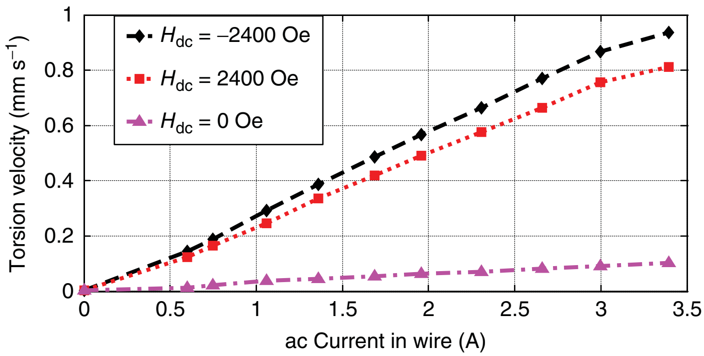

Figure 1.8 Torsion velocity of PZT beam versus ac current in conducting wire.

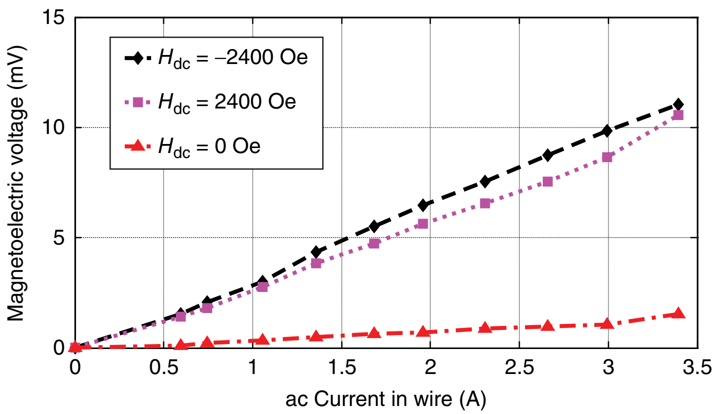

Figure 1.9 ME voltage of PZT beam versus ac current in conducting wire.

velocity versus ac current amplitude were obtained. From the results, the conclusion that the ME response and torsion intensity could be controlled by adjusting the ac current in the conducting wire close to the beam was drawn. Therefore, the dc magnetic field actuating the beam with a linear response and high sensitivity would be achieved with the ac magnetic field applied perpendicularly to the plane of a piezoelectric beam.

The aforementioned experiments of the ME sensor and the magnetic actuator with piezoelectric ceramic have shown that the prototype of the ME sensor and the magnetic actuator without magnetic phase and also without applying power source was promising to be put into practical applications of magnetic field sensing and actuating technology.

1.4 Magnetoelectric Effect in Insulating Polymers

With the advent of science and technology, the performance of the insulating polymers attracted great attention from the researchers. However, little research

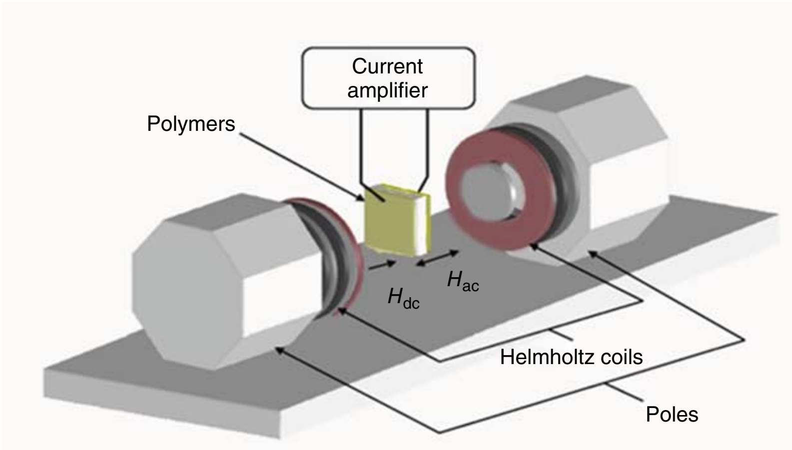

Figure 1.10 ME measurement system [16].

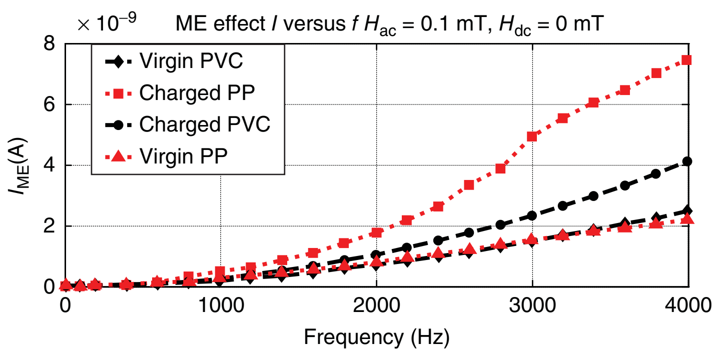

Figure 1.11 Comparison of ME current between discharged and nondischarged porous PP.

work has been done on the comparison of the charge-storage ability among the different electrets by using the ME measuring system. In order to investigate the ME performances before and after high-voltage corona treatment of different electrets, the discharged porous polypropylene (PP) and polyvinyl chloride (PVC) had been chosen in the experiment.

As shown in Figure 1.10, because the ME current was induced by the integrated magnetic field, the suspended piezoelectric samples would be considered as the micro-generator whose ME effect could be suitably amplified by the current amplifier and the current subsequently observed by the oscilloscope.

As shown in Figure 1.11, the ME current in the corona-charged porous PP and PVC is higher than the nondischarged porous PP and PVC. Under the same poling conditions, the corona-charged porous PP possesses a higher ME current compared with the corona-discharged porous PVC.

This phenomenon is observed because the corona poling of the specimen led to the charge injection in the sample surface and volume and then formed a space-charge layer, which augmented the capacitance of the charged films due to the interfacial polarization after corona poling. It is indicated that the porous PP, which possesses better charge-storage ability, can enhance ME effect response. And the charges injected in the polymers can have an effect on the ME effect responses.

The basic element model can be established as follows: the induced eddy currents originate from the applied magnetic field, which induces magnetic flux through the surface measurement of the electrodes S and can be expressed as [15]

$$\varphi = \iint_s B_{ac} \mathrm{d}S \tag{1.1}$$

where B_{ac} is ac magnetic induction vector. Consequently, electromotive forces (emfs: V_{Faraday}) appearing around loops in the metal electrode can be expressed as [17]

$$V_{\mathrm{Faraday}} = -\mathrm{d}\varphi_{\mathrm{loop}}/\mathrm{d}t = -\mathrm{d}B\cdot S/\mathrm{d}t = -j\omega B_{ac}\cdot S = -j\omega\cdot\varphi_{\mathrm{loop}} \tag{1.2}$$

The equivalent circuit of the proposed modeling is as shown in Figure 1.12. In the schematic, the circuit with a capacitance C_p, a resistance R_p, and series with voltage source is equivalent to the sample in the magnetic field. The series with voltage source includes V_{Faraday} and V_{ME}, which are from Faraday effect and ME effect, respectively. R_c is the resistance measured with current amplifier.

The magnetically induced current i_{Lenz} sources of the V_{Faraday} in the circuit can be expressed as [17]

$$i_{\mathrm{Lenz}} = v_{\mathrm{Faraday}}/(Z + R_c) \tag{1.3}$$

Because $Z \gg R_c$, i_{Lenz} can be expressed as [17]

$$i_{\mathrm{Lenz}} = v_{\mathrm{Faraday}}/Z \tag{1.4}$$

where Z is the electrical impedance of the film at the measurement frequency and can be expressed as [17]

$$Z = R_p/(1/jC_p\omega) = R_p/(jC_pR_p\omega + 1) \tag{1.5}$$

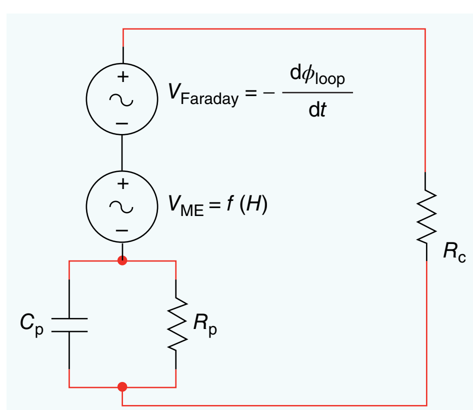

Figure 1.12 Schematic of equivalent circuit. Zhang *et al*. 2014 [17]. Reproduced with permission of Elsevier.

Finally, resolving Eqs (1.2), (1.4), and (1.5) gives the calculated results of the Lenz current I_{Lenz} as follows [17]:

$$I_{\text{Lenz}} = \omega\cdot\varphi_{\text{loop}}(C_p\omega - j/R_p) \tag{1.6}$$

The ME current i_{ME} sources of the V_{ME} in the circuit can be expressed as [17]

$$i_{\text{ME}} = V_{\text{ME}}/Z_c \tag{1.7}$$

where V_{ME} is the ME alternative voltage and can be expressed as [17]

$$\begin{aligned} V_{\text{ME}} &= V_{\text{ME}}(H)|_{H=H_0} + \left.\frac{dV_{\text{ME}}(H)}{dH}\right|_{H=H_0} H + \frac{1}{2}\left.\frac{d^2V_{\text{ME}}(H)}{dH^2}\right|_{H=H_0} H^2 + \cdots \\ &= V_{\text{ME}}(H)|_{H=H_0} + e\times\left.\frac{dE_{\text{ME}}(H)}{dH}\right|_{H=H_0} H + \frac{1}{2}\times e\times\left.\frac{d^2E_{\text{ME}}(H)}{dH^2}\right|_{H=H_0} H^2 + \cdots \\ &= \text{Const} + e\times\alpha_E\cdot H + \frac{1}{2}\times e\times\beta_E\cdot H^2 + \cdots \end{aligned} \tag{1.8}$$

where E_{ME} is the electric field, e the thickness of the sample, α_E the ME voltage linear coefficient, and β_E is second-order ME voltage coefficient. Because the voltage V_{ME} is alternative root mean square (RMS) of the alternative value of ME voltage, Const = 0. And the ME current is a function of H_{dc}, which is a constant (in Figure 1.13), so $\beta_E = 0$.

The total current comes from both the magnetically induced current i_{Lenz} and the ME current i_{ME} [17]:

$$I_t = I_{\text{ME}} + I_{\text{Lenz}} \tag{1.9}$$

Finally, resolving Eqs (1.5), (1.7), and (1.8) gives the calculated results of the Lenz current i_{ME} as follows [17]:

$$I_{\text{ME}} = V_{\text{ME}}/R_p(jC_pR_p\omega + 1) = V_{\text{ME}}(jC_p\omega + 1/R_p) \tag{1.10}$$

And the ME coefficient α_E is [17]

$$\alpha_E = |I_{\text{ME}}|/e\times H\sqrt{(C_p\omega)^2 + (1/R_p)^2} = |I_t - I_{\text{Lenz}}|/e\times H\sqrt{(C_p\omega)^2 + (1/R_p)^2} \tag{1.11}$$

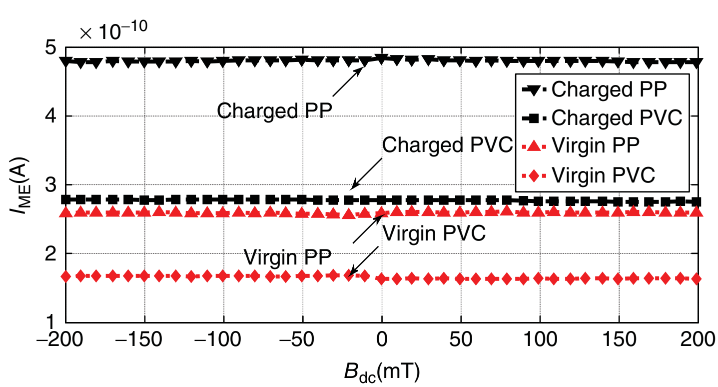

Figure 1.13 Comparison of ME effect between charged and noncharged cellular PP and PVC (@Bac = 0.1 mT, f = 1 kHz).

The investigation of ME performances in comparing the charge-storage ability among different electrets establishes the fact that enhanced ME performance could be achieved by using effective corona poling method on insulator polymers and not just by adding micro- or nano-additives into the specimen.

1.5 Conclusion

In this chapter, the ME effect and its application in single crystal, multilayered composites, and piezoelectric under Lorentz force induced by eddy current were discussed. A generalized ME effect was caused by an ac conducting wire and a piezoelectric beam from which a higher ME voltage coefficient was obtained than previous related research. The ME effects of such a designed piezoelectric beam set a good example of new ME systems without magnetic phase in the sample and also without applying power source on the piezoelectric beam. Magnetoelectric response of the magnetic actuator and the ME sensor composed of different electrets without magnetic phase is promising to be put into practical applications of magnetic field sensing and actuating technology.

Acknowledgments

This work was supported by the Science and Technology Project of State Grid Corporation of China, National Natural Science Foundation of China (NSFC) (Grant No. 51307016), the State Key Laboratory of Engineering Dielectrics and Its Application (Ministry of Education, China), Opening Fund of Key Laboratory of Silicon Device Technology (Chinese Academy of Sciences), and Excellent Young Teachers Program of Northeast Dianli University. The authors would like to extend their sincere gratitude to Ms Feng Yan for her assistance in improving the English text.

References

1 Lu, C., Xu, C., Wang, L., Gao, J., Gui, J., and Lin, C. (2014) Investigation of optimized end-bonding magnetoelectric heterostructure for sensitive magnetic field sensor. *Rev. Sci. Instrum.*, **85** (11), 115003.

2 Yu, X., Lou, G., Chen, H., Wen, C., and Lu, S. (2015) A slice-type magnetoelectric laminated current sensor. *IEEE Sens. J.*, **15** (10), 5839–5850.

3 Dong, S., Liu, J.M., Cheong, S.W., and Ren, Z. (2015) Multiferroic materials and magnetoelectric physics: symmetry, entanglement, excitation, and topology. *Adv. Phys.*, **64** (5-6), 519–626.

4 Leung, C.M., Zhang, S.Y., Or, S.W., Ho, S.L., and Lee, K.Y. (2012) *Proceedings of the 1st International Workshop on High-Speed and Intercity Railways*, Springer, Berlin, pp. 319–327.

5 Fiebig, M. (2005) Revival of the magnetoelectric effect. *ChemInform*, **36** (33), R123–R152.